ACS Chemical Neuroscience
Cite This: ACS Chem. Neurosci. XXXX, XXX, XXX−XXX
Research Article
pubs.acs.org/chemneuro

Neuro-Regenerative Choline-Functionalized Injectable Graphene Oxide Hydrogel Repairs Focal Brain Injury

Krishnangsu Pradhan,[†,§] Gaurav Das,[†,‡,§] Juhee Khan,[†] Varsha Gupta,[†] Surajit Barman,[†] Anindyasundar Adak,[†] and Surajit Ghosh*[,†,‡]

[†]Organic & Medicinal Chemistry Division and [‡]Academy of Scientific and Innovative Research, CSIR-Indian Institute of Chemical Biology, 4 Raja S. C. Mullick Road, Jadavpur, Kolkata 700032, West Bengal, India

Supporting Information

ABSTRACT: Brain damage is associated with spatial imbalance of cholinergic system, which makes severe impact in recovery of damaged neurons of brain. Therefore, maintenance of cholinergic system is extremely important. Here, we fabricated an injectable hydrogel with acetylcholine-functionalized graphene oxide and poly(acrylic acid). Results revealed that this hydrogel is non-cytotoxic, promotes neurite outgrowth, stabilizes microtubule networks, and enhances the expression of some key neural markers in rat cortical primary neurons. Further, this hydrogel exhibits significant potential in neuro-regeneration and also promotes fast recovery of the sham injured mice brain. Moreover, we found significant enhancement of reactive astrocytes in the hippocampal dentate gyrus region of the sham injured brain, indicating its excellent potential in neural repair of the damaged brain. Finally, above results clearly indicate that this neuro-regenerative hydrogel is highly capable of maintaining the cholinergic balance through local release of acetylcholine in the injured brain, which is crucial for brain repair.

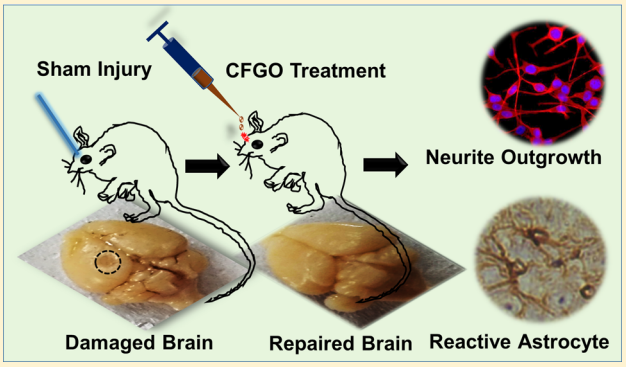

KEYWORDS: *Acetylcholine, Graphene oxide, Injectable hydrogel, Neurite outgrowth, Brain injury, Neuroprotection*

1. INTRODUCTION

Brain is an epicenter of all major complex biochemical activities that has mesmerized scientists for eras.[1,2] This enigmatic machinery is a highly sophisticated and extremely complex network structure consisting of millions of neurons and glial cells that interconnect to give rise to the intellects.[3] It acts as an essential integrated system, which controls all the physiological, motor, and cognitive functions. Slight perturbation or damage to this complex array of system leads to severe complications of its essential functions.[4] The major concern with this complex machinery is its limited regenerative capabilities, and due to this fact adopting novel approaches to understand the repair mechanism is extremely important.[5] Recently, various attempts such as stem cell-based regeneration have been made toward this extremely complex issue.[6] However, none of those approaches have been translated into any clinical success.[7] Therefore, to address this complex issue many novel strategies like fabrication of potential biomimetic scaffolds such as electrospun fibers, hydrogels,[8] and various chemically functionalized carbon-based materials have been conceived.[9] Graphene-based materials (GO)[10−12] have attracted huge attention for the fabrication of various biomaterials due to their excellent electrical, chemical, thermal, and charge carrier properties along with negligible electrical noise, low toxicity, and high biocompatibility.[13,14] Interestingly, unique electrical properties[15] of graphene oxide have been utilized for studying neural growth as well as neural stimulations.[16] Acetylcholine plays a crucial role, as it maintains cortical activation,[17] synaptic function,[18] neuroprotection,[19,20] neurogenesis,[21] cortical differentiation,[22,23] neuronal plasticity,[24] and cortical reorganization.[25,26] During brain injury, cholinergic system is severely damaged. It has been shown that cholinergic system plays a crucial role in cortical plasticity and functional recovery after brain injury.[27] Therefore, maintaining the choline balance in injured brain tissue is crucial for the successful repair of damaged brain.[28] So far a few attempts have been made toward maintenance of choline balance in damaged brain.[29] Herein, we adopted a simple but potential approach to maintain the choline balance in the damaged brain using covalently conjugated choline-graphene oxide nanomaterials.

2. RESULTS AND DISCUSSION

2.1. Synthesis of CFGO-Based Hydrogel. For the functionalization of the graphene oxide, 2-hydroxy-*N*′,*N*′,*N*′-trimethylethanaminium was prepared from 2-aminoethanol and conjugated with GO (Figures S1 and S2). Then, we prepared a novel injectable hydrogel[30,31] using this choline-

Received: September 28, 2018
Accepted: November 14, 2018
Published: November 14, 2018

DOI: 10.1021/acschemneuro.8b00514
ACS Chem. Neurosci. XXXX, XXX, XXX−XXX

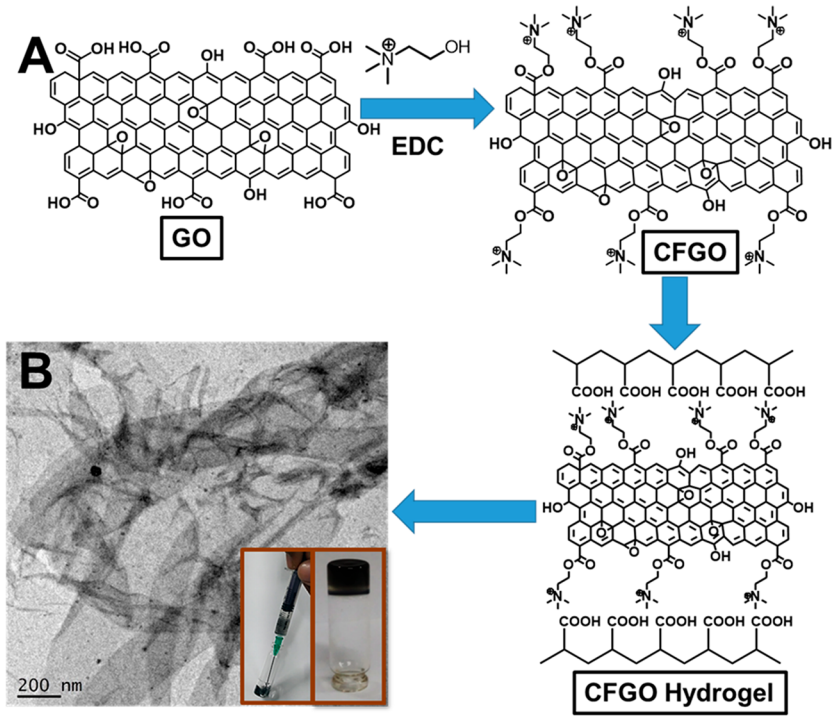

Figure 1. Synthesis and charecterization of CFGO-based hydrogel. (A) Synthetic scheme for preparation of CFGO hydrogel. (B) TEM image of CFGO hydrogel. (inset, right) Hydrogel formation and (inset, left) the injectable property.

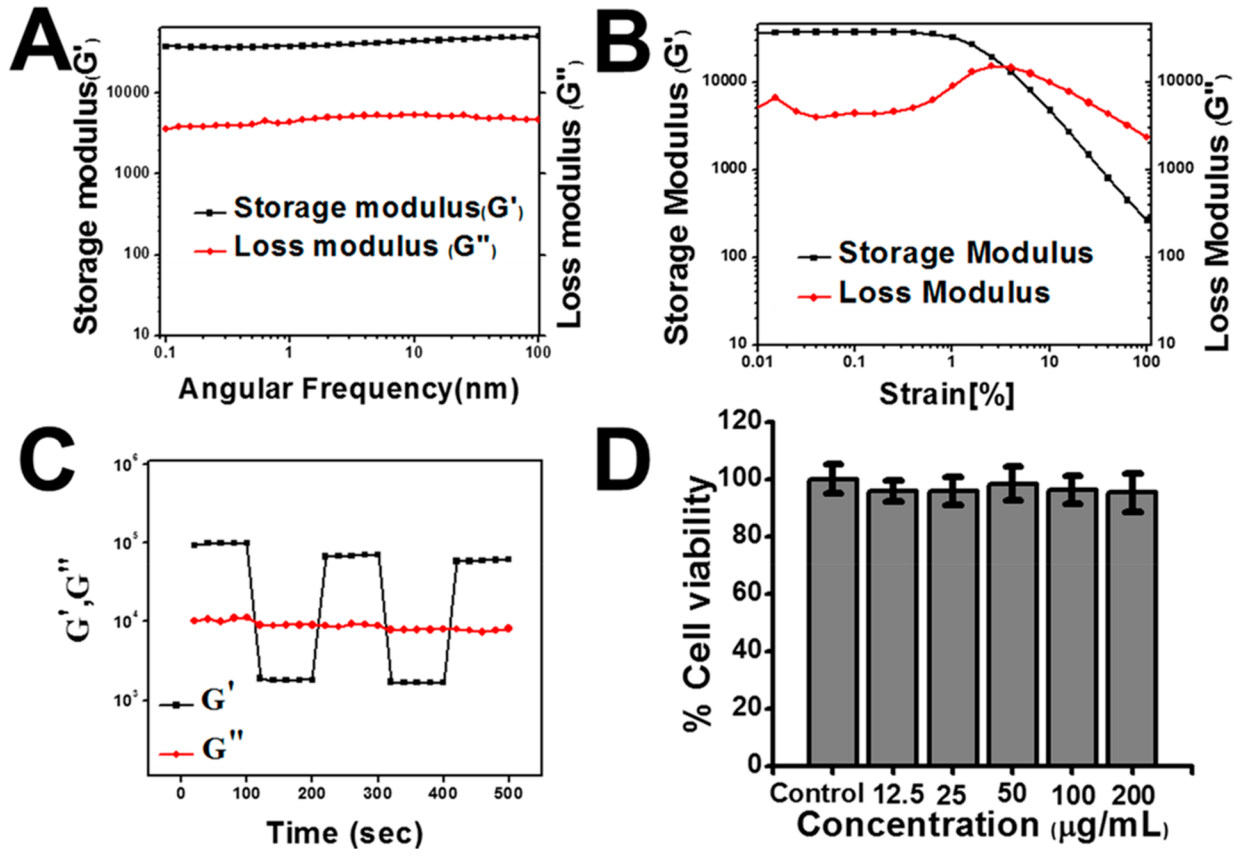

Figure 2. Rheological analysis and MTT assay of CFGO-based hydrogel. (A) Frequency sweep rheology of CFGO hydrogel. (B) Strain sweep curve of CFGO hydrogel. (C) Thixotropic study of CFGO hydrogel. (D) Cytotoxicity assay of CFGO hydrogel.

graphene oxide nanomaterial with poly(acrylic acid) (CFGO) (Figure 1A).

2.2. FT-IR Spectroscopy for Characterization of CFGO. GO and CFGO were characterized by Fourier transform

DOI: 10.1021/acschemneuro.8b00514
ACS Chem. Neurosci. XXXX, XXX, XXX−XXX

infrared (FT-IR) spectroscopy. For that purpose, GO and CFGO samples were lyophilized to get the powder. The data were recorded using FT-IR JASCO FT-IR 4200 model. The FT-IR spectrum of GO reveals peak at 882 cm^{-1} signifying the presence of epoxy group in the GO surface. The peak at 1115 cm^{-1} for GO signifies C−OH stretching frequency of −COOH group supporting the presence of −COOH group in GO surface.[32] The peak at 1720 cm^{-1} due to carbonyl stretching of the carboxyl group also supported the presence of −COOH group in GO surface. But in case of CFGO, the characteristic peak at 1735 cm^{-1} due to ester bond supports covalent functionalization on GO and formation of CFGO.[32] Peaks at the region from 3000 to 3700 cm^{-1} for both the cases are due to O−H stretching (both free and H-bonded) and amide N−H bond (secondary) stretching (Figure S3).

2.3. UV−Vis Spectroscopy for Characterization of CFGO. UV spectroscopy was used to characterize GO and CFGO. The UV spectroscopy results revealed that the characteristic absorption peaks appear at 234 and 300 nm, which signify the formation of GO. But for CFGO a similar spectral analysis results in the reduction in intensity of the peak at 234 nm, which supports the functionalization of the GO surface and formation of CFGO (Figure S4).

2.4. X-ray Photoelectron Spectroscopy (XPS) for Characterization of CFGO. The formation of CFGO was further confirmed by XPS measurements. In the wide-scan spectrum of CFGO, carbon (C 1s at 284.6 eV), nitrogen (N 1s at 402.2 eV), and oxygen (O 1s at 532.0 eV) signals appeared (Figure S5). This result indicates that acetylcholine mimicking functional group is successfully covalently attached onto the GO sheets. Further evidence for the formation of CFGO was obtained through high-resolution XPS spectra. The high-resolution XPS spectra of C 1s for CFGO (Figure S6A) revealed peaks at 284.6 eV (C−C), 286.7 eV (C−O, C−N^+), and 288.7 eV (O−C═O). Atomic percentage of each group of the CFGO was also calculated. The result showed that C−C was 56.2%, C−O, C−N^+ was 29.5%, and O−C═O was 14.3% (Figure S6B). The high-resolution XPS spectra of N 1s showed peak at 402.4 eV for C−N^+ peak (Figure S7). These informations also support the successful functionalization of acetylcholine on the GO surface. These XPS results also suggest that the CFGO nanocomposite was successfully prepared.

2.5. Transmission Electron Microscopy for Characterization of CFGO Hydrogel. CFGO hydrogel was characterized by transmission electron microscopy (TEM). TEM image of the CFGO hydrogel shows the presence of a three-dimensional (3D) network structure comprising of self-assembled large nanosheets (Figure 1B).

2.6. Rheological Study for CFGO Hydrogel. Viscoelastic behavior of the CFGO-based hydrogel was analyzed by rheological analyses in terms of storage modulus (G') and loss modulus (G''). Hydrogels are generally characterized by a "solid-like" behavior, and the storage modulus is much higher than the loss component. Frequency sweep experiment of the hydrogel reveals that both G' and G'' remain independent in the frequency range from 0.1 to 100 rad/s ($G' > G''$; Figure 2A). This result also supports the solid-like rheological behavior of the CFGO hydrogel. To get better information about the yield stress of the CFGO-based hydrogel, the amplitude sweep experiment was performed. The maximum yield stress of the CFGO hydrogel was ∼6 kPa (Figure 2B). To analyze the thixotropic behavior of CFGO, step-strain experiment was performed. When the strain is applied above the linear viscoelastic (LVE) region, the hydrogel loses its solid-like behavior ($G' < G''$). But the sol form of the hydrogel quickly goes back to the solid-like state ($G' > G''$) when the strain is applied to the LVE region of the CFGO hydrogels (Figure 2C). This thixotropic property demonstrates that CFGO hydrogel has a great character to recover the gel-like property, which is crucial for injectable applications of the hydrogel.

2.7. Injectable Nature of CFGO Hydrogel. Hydrogel gains a lot of attention in the medicinal field due to its injectable nature. Injectable hydrogels can easily be delivered to the target region in vivo via a simple syringe without giving the pain of surgical treatment to the patient. Therefore, we checked the practical applicability of this type of hydrogel; that is, whether they are injectable or not. The injectable nature of the hydrogel was checked with a syringe. The images revealed that hydrogel can be injected through a syringe and removed from the syringe as a sol (Figure S8). After some time, the sol is converted to the gel automatically.

2.8. Biocompatibility and Neurite Outgrowth of PC12-Derived Neurons on CFGO Hydrogel. The growth of the PC12-derived neurons on the biomimetic CFGO hydrogel was assessed by plating cells on the surface of an overnight UV-sterilized hydrogel coated on the surface of the glass slides. Following this, the cells were cultured for 7 d on these gels and found to retain healthy morphology while promoting neurite outgrowth. For a control setup, cells were grown on CFGO uncoated glass coverslips. Before proceeding any further, it was important to know the biocompatibility of CFGO; the PC12 cells were cultured and differentiated into neurons in the presence of NGF. Then, the neurons were treated with CFGO at various concentrations up to 200 μg/mL. 3-(4,5-Dimethylthiazol-2-yl)-2,5-diphenyltetrazolium bromide (MTT) assay was performed to check the cell viability; CFGO did not exert any cytotoxic effects (Figure 2D). This high cell viability of the PC12-derived neurons even after the treatment with CFGO indicated that CFGO possess excellent biocompatibility for neuron culture. The various neuronal morphological characteristics (no. of branches, mean neurite length, cell body area, and maximum neurite length) as indicated in the figure were quantified using the CellSens software. It was found that the number of branches, the area of the cell body, the maximum and mean lengths of neurites of the PC12-derived neurons grown on CFGO were significantly higher than those grown on GO-coated or (control) uncoated coverslips (Figure 3A−E). The health of the neurons was further confirmed through daywise increase in expression of neuronal marker GAP 43 (Figure S9). All the above results indicate that our CFGO hydrogel promoted growth, proliferation, and health of the neurons. Microtubules are one of the key cytoskeletal filaments of the cells responsible for the various cargo transports. These microtubules are particularly very important in context of neurons, as without these filaments the neurons would not be able to maintain their exaggerated shape. Along with the maintenance of the dynamicity of the neuronal architecture, they regulate the transport of cargo proteins along its long axon and dendrites. It is due to this reason that the microtubule arrays are tightly organized in axons, dendrites, growth cones, and migratory neurons with respect to their intrinsic polarity, which is important for both their assembly and transport mechanisms.[33] These inexplicably important roles of microtubules in neurons

DOI: 10.1021/acschemneuro.8b00514
ACS Chem. Neurosci. XXXX, XXX, XXX−XXX

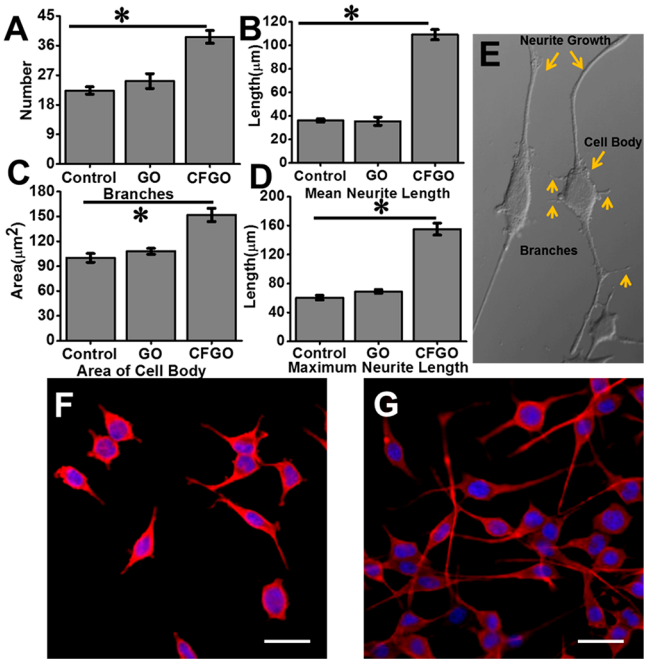

Figure 3. Neurite outgrowth of PC12-derived neurons cultured on CFGO hydrogel. Various parameters of PC12-derived neurons after 7 d of culture on CFGO hydrogel. (A) Branches. (B) Mean neurite length. (C) Cell body area. (D) Maximum neurite length. (E) DIC image showing neurite growth, cell body, and branches. Images of PC12-derived neurons stained with α-tubulin. (F) Control cells. (G) cells grown on CFGO hydrogel. Scale bars correspond to 20 μm.

prompted us to check whether our choline-functionalized hydrogel was able to confer stability to the microtubule networks in the PC12-derived neurons or not. The 7 d old differentiated neurons grown on CFGO-coated coverslips were stained with anti-alpha tubulin antibody and analyzed under the microscope. Microscopic images revealed that, in comparison to neurons grown on uncoated coverslips, the neurons grown on CFGO hydrogel were not only healthy but also showed microtubule stabilization (Figure 3F,G and Figures S10 and S11).

2.9. Actin Filament Stabilization of PC12-Derived Neurons on CFGO Hydrogel. Since CFGO-based hydrogel promoted microtubule stabilization, we checked its effect on another important cytoskeletal filament, actin. Actin is a highly conserved protein that takes part in many protein−protein interactions and carries the inherent ability to transition between monomeric (G-actin) and filamentous (F-actin) states controlled by nucleotide hydrolysis and a group of actin-binding proteins. Thus, actin participates and regulates a host of cellular functions like cell motility, maintenance of cell shape, and polarization of transcription regulation. Actin filaments of the neurons cultured on the CFGO hydrogel-coated glass cover slides were stained with Alexa Fluor 488 phalloidin. Phalloidin is a rigid bicyclic heptapeptide of phallotoxin class isolated from the Amanita phalloides "death cap" mushroom, which selectively labels F-actin and can be used for imaging actin filaments. Microscopic images revealed that CFGO hydrogel promoted healthy network of actin filaments, and hence this CFGO hydrogel can be regarded as a cytoskeleton stabilizer (Figure S12). This exhibits the multifunctional nature of CFGO hydrogel, whereby along with promotion of neurites, they also confer stability to their cytoskeleton framework.

2.10. The Growth and Culture of Primary Rat Cortical Neurons on CFGO Hydrogel. In our earlier observations, it was noted that CFGO hydrogel promoted the growth and attachment of PC12-derived neurons. Therefore, we decided to check how the primary rat cortical neurons would behave when plated on CFGO hydrogel-coated coverslips. For this purpose, primary cortical neurons were isolated from the cortex of Sprague−Dawley embryonic day 18 rats and plated on the CFGO hydrogel-coated coverslips. It was observed that the rat cortical neurons attached and grew on these coverslips for the next 14 d. Their growth on the CFGO surfaces over the next 14 d was marked by extensive neurite outgrowths and numerous dendritic projections, mostly resembling morphological features observed in cortical neurons in situ (Figure S13). Since CFGO hydrogel has already shown microtubule stability, we stained the primary cortical neurons with Microtubule Associated Protein 2 (MAP2), a neuron-specific cytoskeletal protein, highly enriched in dendrites with a significant role in microtubule assembly that promotes stabilization of the dendritic shape during neurogenesis. The MAP2-stained images of the primary cortical neurons cultured on CFGO hydrogel indicated the ability of the gel to promote the neuronal morphology of the cortical neurons along with additional stability to its microtubule network (Figure 4A,B).

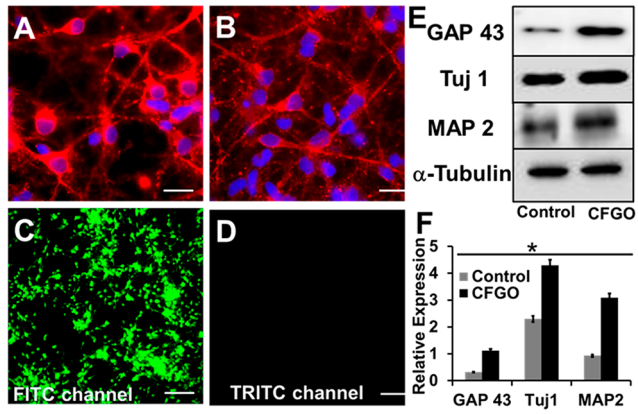

Figure 4. Neurite outgrowth and live dead cell assay of primary cortical neurons cultured on CFGO hydrogel. Microscopic images of primary cortical neuron (A) control. (B) Neurons cultured on CFGO hydrogel. Live dead cells assay of primary cortical neurons cultured on CFGO hydrogel in (C) fluorescein isothiocyanate (FITC) channel, (D) tetramethylrhodamine isothiocyanate (TRITC) channel. Scale bars correspond to 20 μm. (E) Western blot experiment of various markers of neuron. (F) Quantitative analysis of various neuron markers.

Next, we checked the biocompatibility of the CFGO by performing the live dead cell assay using calcein AM/propidium iodide (PI) on the primary cortical neurons cultured on CFGO. Microscopic images revealed that even after 14 d of culture the neurons retained almost 100% cell viability, indicating that CFGO possesses good biocompatibility for cortical neuron culture (Figure 4C,D). In our previous studies, we observed that, along with PC12-derived neurons, CFGO also promoted the growth and differentiation of primary rat cortical neurons. This led us to check the expression of three key neuronal markers—Growth Associated Protein 43 (GAP 43), β-tubulin-III (Tuj 1), and MAP2 in the

DOI: 10.1021/acschemneuro.8b00514
ACS Chem. Neurosci. XXXX, XXX, XXX−XXX

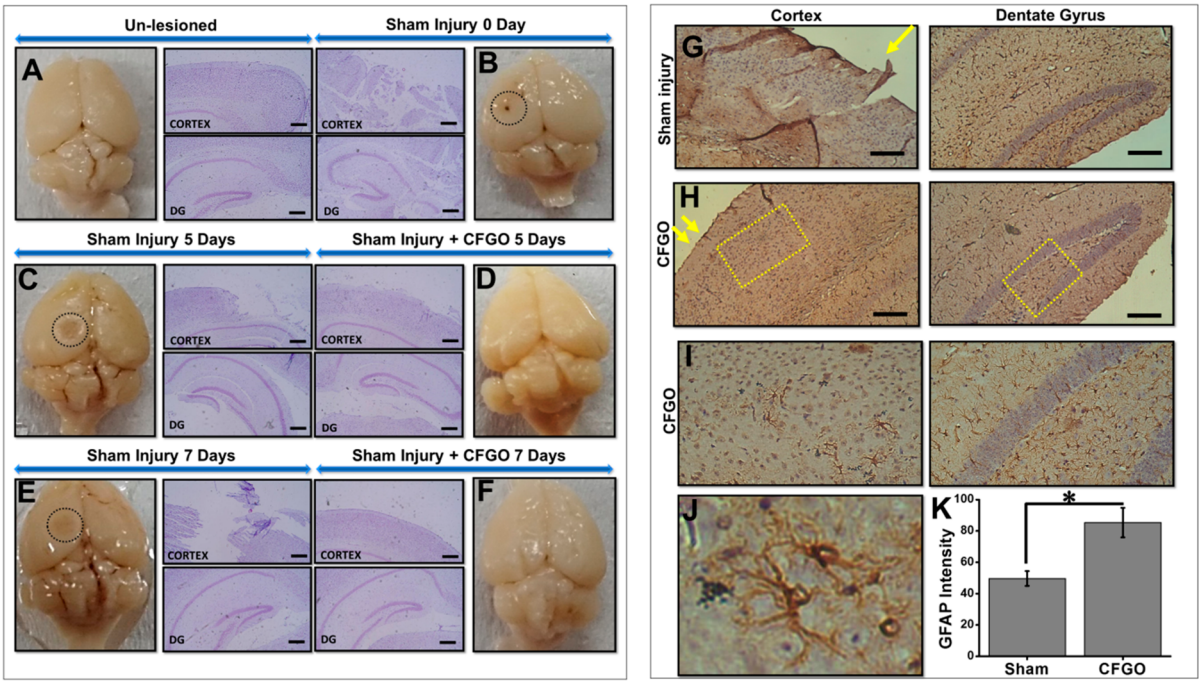

Figure 5. Repairing of sham injury in the mice brain with the treatment of CFGO hydrogel. Physical appearance of brain and cresyl violet staining of cryogenic injury of mice brain showing cortex and DG region of hippocampus (A) Unlesioned. (B) Sham injury at 0 d. (C) Sham injury at 5 d. (D) Sham injury at 7 d with CFGO. (E) Sham injury at 7 d. (F) Sham injury at 7 d with CFGO. Immunohistochemical study of GFAP expression in cortex and dentate gyrus region (G) Sham injury (single arrow signifies site of injury). (H) Sham injury with CFGO at 7 d (double arrow signifies recovery from the injury). (I) Magnified images of (H). (J) Magnified image of reactive astrocytes. (K) Quantitative assessment of GFAP expression in the DG region.

primary cortical neurons cultured on the CFGO coated plates. GAP 43 is also known as the "growth" or "plasticity" protein, as it is highly expressed in developing or regenerating neurons during axon growth. Tuj 1 is a class III member of the β-tubulin protein family, specifically localizes to neurons having implications in neurogenesis, axon guidance, and maintenance. MAP 2 as already discussed indicates microtubule stability and dendritic growth in neurons. To investigate the expression of these key neuronal proteins, those were isolated from the primary cortical neurons and cultured on CFGO hydrogel for 14 d, and subsequently immunoblot analysis was performed with the respective primary antibodies. It was observed that the expression of all three neuronal markers (GAP 43, MAP2, and Tuj1) were higher in the neurons cultured on CFGO hydrogel as compared to those cultured on uncoated surfaces (Figure 4E). These results indicate that the CFGO hydrogel promotes neuronal outgrowth and sprouting through the upregulation of the key neuronal markers (Figure 4F).

2.11. Effect of CFGO on Focal Cryogenic Injury at the Parietal Cortex of C57BL/6J Mice Brain. Both components of our CFGO hydrogel, graphene oxide and choline, have neuroprotective roles. Of them, especially, choline is known to exert neurogenesis in an injured brain and has been evaluated for its potential of neuro-recovery in the treatment of stroke as well as Traumatic Brain injury (TBI) in various animal models and human clinical trials.[34,35] On the basis of all the observations made so far with PC12-derived neurons and primary rat cortical neurons, CFGO seems to also have neuroprotective activity, which should be further validated in animal models. Therefore, in our next study we tried to understand the neuroprotective role of CFGO in cryogenic injury model (CIM) of mice. Unilateral cryogenic lesions is a type of focal injury made on the exposed skull bone of the parietal cortex with a copper rod having a tip diameter of 2.5 mm cooled in liquid nitrogen. For our study, we used C57BL/6J male mice and divided them into three groups each having five mice (n = 5) (Unlesioned control, Control Sham injury, and sham injury to be treated with CFGO). Thereafter, we performed a focal injury in the parietal cortex following the cryoinjury technique. In the third group of mice, CFGO was applied over the cryolesion, and the mice brains were isolated following the fifth and seventh days of treatment through transcardial perfusion. Similarly, lesioned and unlesioned brains were isolated from the sham injury and unlesioned control mice groups, respectively. The brains were then fixed in 4% formalin, and images were taken. On careful examination, a distinct focal injury was observed in the mice brain, which persisted in the sham injured mice up to 7 d, while absence of any such cryolesion in the CFGO treated brains indicated complete recovery. For the histopathological studies, 5 μm thick coronal sections of the brain were taken and stained with cresyl violet. Cresyl violet acetate stains Nissl substances in the cytoplasm of formalin-fixed neurons and are commonly used to identify neuronal structures in brain and spinal cord tissue. Cresyl violet stains indicated cortical loss in the brains of sham injured mice taken at three different time points (0, 5, and 7 d), while no such cortical loss was observed in the CFGO-treated mice brains treated for 5 and 7 d, indicating its potential for neuro-recovery. The unlesioned control mice brain also showed no such cortical cell loss. No cell loss was observed in the ipsilateral dentate gyrus (DG) region in any of the mice brain sections indicating the focal nature of our injury. All the above observations indicate the neuroprotective nature of CFGO hydrogel in injured mice brains (Figure 5A–F). Cryogenic

DOI: 10.1021/acschemneuro.8b00514
ACS Chem. Neurosci. XXXX, XXX, XXX−XXX

injury in the brain leads to a cascade of events that result in severe neuroinflammation and neuronal cell death. In response to such injury, the astrocytes become reactive exhibiting hypertrophy and hyperplasia. These bunches of reactive astrocytes have been shown to play essential roles in preservation of neural tissue and reduction of neuroinflammation after a focal injury by forming a glial scar. Reactive astrocytes are marked by an elevated expression of Glial Fibrillary Acidic Protein (GFAP), a cell-specific marker for astrocytes. In our study, we tried to evaluate the protective role of these reactive astrocytes by performing immunostaining of GFAP in the coronal sections of the fixed brains. A number of hypertrophoid astrocytes were observed in the cortical region of the CFGO-treated brain sections as could be seen from the enlarged image, which promotes the protective nature of our hydrogel (Figure 5G–I). Moreover it is well-documented that neurogenesis and cell proliferation increases in the hippocampal DG region after injury, which is a potential source of neurons for repair. Hence, we calculated the number of astrocytes in the DG region from the 7 d CFGO-treated and sham injured mice brain sections; it was found that there is a higher expression of GFAP in the CFGO-treated mice indicating speedy recovery (Figure 5K). This result further validates the potential role of our CFGO gel in neuro-recovery following injury.

3. CONCLUSIONS

The brain although an incredible organ comes with its own weaknesses; for example, it struggles to repair itself after sustaining damage from injury or stroke. This limited regenerative potential of the brain prompted us to design an acetylcholine-functionalized graphene oxide hydrogel due to the ionic interaction of positive charge of the quaternary amine with the negative charge of the poly(acrylic acid). Acetylcholine is known to be an essential neurotransmitter. Previously, various neurotransmitters have shown potential in regulating neuronal development and enhancing neurite outgrowth. The studies with PC12-derived neurons revealed that CFGO hydrogel is biocompatible with neurons, can be used to prolong culture up to 7 d with no additive cyto-toxicity, and promote neurite branching vigorously. This experiment first gave us the idea of the importance of its neurotransmitter mimicking functional group and how it potentiates its neurogenic attributes. Next, we also cultured primary rat cortical neurons on CFGO, and it was observed up to 14 d of culture the neurons showed almost 100% biocompatibility. Along with that, CFGO also leads to an increase in the expression of some key neuronal markers like GAP43, Tuj1, and MAP2, thereby proving that CFGO promotes growth of the primary cortical neurons. CFGO was additionally found to stabilize key cytoskeletal filaments, microtubules, and actin of the neurons, which help in structure maintenance and intracellular/axonal transport. Along with this, our neuro-regenerative gel showed injectable property, and therefore we treated it with a sham injured mice brain at the site of cryolesion. To our surprise, our hydrogel showed almost full recovery of the injury within 5 and 7 d of treatment. This was more clearly observed through cresyl violet staining of the brain slices. At the DG region of the brain slices, a larger number of reactive astrocytes in the treated mice brain further indicated its neuro-regenerative potential. This result is supported by measuring the GFAP expression, which signifies the reactive astrocytes in the hippocampal DG region of the injured brain. Overall, these findings support that acetylcholine-functionalized graphene oxide-based hydrogel may be considered as an excellent platform for neuronal outgrowth and neuron repair in the mice model.

4. EXPERIMENTAL SECTION

4.1. Chemicals. Graphite powder (<60 μm) was bought from Loba Chemie. Trifluoroacetic acid (TFA) was purchased from Spectrochem. Potassium permanganate and sodium hydroxide were purchased from Fisher Scientific. Sodium nitrate, sulfuric acid, hydrogen peroxide (30%), and potassium carbonate were purchased from Merck. Dry methanol was purchased from Acros Organic. 2-Aminoethanol was purchased from Sigma-Aldrich. Methyl iodide was purchased from Spectrochem. *N*-(3-(Dimethylamino)propyl)-*N*′-ethylcarbodiimide hydrochloride (EDC), MTT, β-mercaptoethanol, kanamycin sulfate, nerve growth factor (NGF) 7S, formaldehyde solution (36%), 2,2,2-tribromoethanol, 4-(2-hydroxyethyl)-1-piperazineethanesulfonic acid (HEPES) buffer, sodium bicarbonate, and low-glucose Roswell Park Memorial Institute (RPMI) 1640 medium were purchased from Sigma-Aldrich. Fetal bovine serum (FBS), horse serum, phosphate-buffered salinle (PBS), pH 7.4, GlutaMAX Supplement, B27 supplement, neurobasal medium, MAP2 Monoclonal Antibody (M13), Hank's Balanced Salt Solution (HBSS), Minimum Essential Medium (MEM), and Penicillin-Streptomycin solution were purchased from Invitrogen. Primary antibodies such as anti-Beta III Tubulin, anti-GAP 43, anti-α-Tubulin (Clone DM1A) and secondary antibodies goat anti-Mouse IgG (H+L) Cy3 conjugate, goat antimouse, and antirabbit IgG antibody (H+L) HRP conjugates were purchased from Merck Millipore. Alexa Fluor 488 Phalloidin was purchased from Thermo Fisher Scientific. Poly(vinylidene fluoride) (PVDF) membrane of 0.45 μm size, bovine serum albumin (BSA), Triton-X 100, and Tween 20 were purchased from Merck Millipore. Glycine, Tris-base, sodium dodecyl sulfate (SDS), cresyl violet stain, ammonium persulfate, tetramethylethylenediamine (TEMED), and bromophenol blue were purchased from Himedia. Surgicals (scalpel, hemostats, scissors, forcep, suture needle, and thread) and copper rod (3.4 mm) were procured locally. Propidium iodide and calcein AM were purchased from BD Biosciences. GFAP antibody (GF5) was purchased from Abcam. UV data were recorded on UV-1800 ENG 240 V Shimadzu model, and FT-IR data were recorded on JASCO FT-IR 4200 model.

4.2. Preparation of 2-Hydroxy-*N*′,*N*′,*N*′-trimethylethanaminium from 2-Aminoethanol. 250 μL of 2-aminoethanol and 20 mL of dry methanol were mixed under nitrogen atmosphere in a two-necked round-bottom flask. Anhydrous potassium carbonate (K_2CO_3, 2 g) was added into the round-bottom flask. Next, methyl iodide (500 μL) was added dropwise into the solution while stirring, and the solution was stirred overnight at room temperature followed by evaporation of solvent to get the product.

4.3. Preparation of CFGO from GO. The graphene oxide was prepared from the commercially available graphite powder (<60 μm) following the modified Hummers method.[36] Then, the graphene oxide was dissolved in Milli-Q water by ultrasonication. The sonication was performed for an hour, and concentration of the solution was maintained at 4 mg/mL. After that, the solution was treated with 3 M aqueous NaOH solution in a round-bottom flask. The solution was sonicated for an additional 3 h. Then, the alkaline solution was neutralized (pH 7.0) using dilute HCl solution. The solution was filtered through Whatman 40 filter paper, and the residue was washed with Milli-Q water several times to get pure graphene oxide (GO–COOH) residue. For the functionalization of the graphene oxide, the preformed 2-hydroxy-*N*′,*N*′,*N*′-trimethylethanaminium (100 mg) was added into the 10 mL GO–COOH solution. The concentration of the graphene oxide solution was maintained at 1 mg/mL. Then the solution was sonicated for 5 min. To the mixture of the solution, EDC was added to reach 5 mM concentration and again sonicated for 30 min. Then, EDC was added into the reaction mixture to reach 20 mM concentration. This reaction mixture was left stirring overnight at room temperature. After it was stirred, 50 μL of β-

DOI: 10.1021/acschemneuro.8b00514
ACS Chem. Neurosci. XXXX, XXX, XXX–XXX

mercaptoethanol was added to the mixture to terminate the reaction. After completion of the reaction, the reaction mixture was centrifuged for 10 min at 12 000 rpm, and washing was performed with milli-Q water 4−5 times. Finally, the residue was lyophilized, and dried CFGO was stored at room temperature.

4.4. UV−Vis Spectroscopy. For this experiment, a solution of GO and acetylcholine-functionalized GO (CFGO) was prepared in Milli-Q water. Then, UV spectra of these solutions were measured maintaining the concentration of the solution at 2 mg/mL.

4.5. FT-IR Spectroscopy. FT-IR spectra of GO and CFGO were measured using KBr pellet. GO and CFGO solutions were lyophilized to get powder compound. Then, these powder compounds were mixed with KBr to prepare the KBr pellet. FT-IR data were recorded in a PerkinElmer Spectrum 100 FT-IR spectrometer through 48 times scan using the above KBr pellets with speed 0.2 cm/s at a resolution of 1.6 cm^{-1}. The $LiTaO_3$ detector was used for plotting the data. For each sample, background correction was performed to eliminate interference from air (or any other parameters).

4.6. X-ray Photoelectron Spectroscopy (XPS). For this analysis freshly prepared CFGO was used. The sample was drop-casted on a glass cover slide. Then, the glass slide was put in a vacuum chamber to remove the solvents. All the XPS analyses were performed using an Al X-ray source operated at 150 W on an Axis Ultra X-ray photoelectron spectrometer. The experiments were performed at an electron takeoff angle of 90°. General survey scan was performed over the binding energy range of 200−800 eV, and high-resolution spectra were recorded in the regions of C 1s, N 1s.

4.7. Preparation of CFGO-Based Hydrogel. For the preparation of CFGO-based hydrogel, a stock solution of poly(acrylic acid) was prepared by dissolving 4 mg in 1 mL of water, and another stock solution of CFGO was also prepared by dissolving 8 mg of CFGO in 1 mL of milli-Q water. Then, in the 10 sets vial we mixed poly(acrylic acid) with CFGO in different proportions. But, when 0.2 mL of poly(acrylic acid) solution was added into the solution containing 0.8 mL of CFGO solution, hydrogel was formed easily. This is the optimized concentration for the hydrogel formation. To form the hydrogel, mixture was heated and occasionally sonicated for 15 min. Then the mixture was kept at room temperature for 30 min to form the CFGO-based hydrogel.

4.8. Rheology. TA Instrument rheometer was used to perform rheology experiments with a cone−plate (diameter 40 mm and angle 4°). All the experiments were performed at a constant temperature (25 °C). The temperature was maintained using a Peltier. For these studies, fresh samples were used. The amplitude and frequency sweep analyses were performed with a fixed gap value. Thixotropic experiments were performed by applying successive deformation and recovery steps. The steps were performed repeatedly at a fixed frequency of 1 rad/s.

4.9. Transmission Electron Microscopy (TEM). For this experiment, a 20 μL CFGO hydrogel was dissolved in milli-Q water (80 μL) by sonication. Then, 10 μL of suspensions solution was placed on a carbon-coated copper grid. After 1 min, excess solution was removed by filter paper, and the grid was stained with 2% uranyl acetate in water. After 1 min of staining, excess uranyl acetate solution was removed with filter paper from the grid. Then, the grids were dried under vacuum. Images were captured using a TECNAI G2 Spirit Biotwin Czech Republic 120 kV electron microscope operating at 80 kV.

4.10. Cell Culture. Rat pheochromocytoma cells (PC12) was a kind gift from Dr. S. N. Bhattacharyya. The cells were cultured in RPMI medium supplemented with 10% heat inactivated horse serum (HS), 5% heat inactivated FBS, 100 units/mL penicillin, and 100 μg/mL streptomycin in a humidified atmosphere with 5% CO_2 at 37 °C. For differentiation into neurons, PC12 cells were treated with nerve growth factor (NGF; 100 ng/mL) in RPMI medium supplemented with 1% HS for 7 d.

4.11. Cell Viability Assay. To assess the biocompatibility of our hydrogel, undifferentiated PC12 cells were plated on 96-well plates and then differentiated for 7 d. Then, the cell viability was checked by MTT assay in PC12-derived neurons. Approximately 5000 cells were seeded per well (total medium volume of 100 μL). After 24 h, postseeding, the medium was replaced with solutions of different concentrations of hydrogel compounds to each well (five wells for each concentration). The MTT assays were performed. Cells without treatment were used as the control.

4.12. Neurite Outgrowth Assay.[37] To assess neurite outgrowth on CFGO hydrogel surfaces, coverslips were coated with CFGO hydrogel, and another set of coverslips were coated with only GO. Then, the PC12 cells were plated on these CFGO and GO surfaces. The cells were then differentiated with NGF over the next 7 d, and their neurite outgrowth was monitored. As control experiment, PC12 cells were plated on uncoated coverslips. Consequently, after 7 d the cells were fixed with 4% formaldehyde and analyzed under microscope (Olympus) in DIC mode. The cells were mainly characterized using four parameters, namely, number of branches, mean neurite length, cell body area, and maximum neurite length. Evaluation of these parameters was performed using the analysis and calculation mode of CellSens software. The quantitative data were presented as the mean ± standard deviation (SD). Tests of data significance were performed using one-way ANOVA.

4.13. Microtubule Stability through Immunostaining. To check whether our hydrogel confers stability to microtubules, a very important component of neuronal cytoskeleton, the PC12 cells were plated on CFGO-coated coverslips and cultured over the next 7 d with NGF to induce them into neurons. Similarly, for control experiments the cells were plated on uncoated coverslips and cultured on them. After 7 d of culture, the cells were first fixed with 4% formaldehyde for 30 min at room temperature and permeabilized using 0.2% Triton X-100 for another 15 min. The permeabilized neurons were incubated with mouse anti-α tubulin overnight at 4 °C. The neurons were then washed with PBS and further incubated with fluorescence-labeled secondary goat antimouse antibody for 2 h at 37 °C. The neuronal nuclei were finally stained with Hoechst dye H33258 (0.05 mg/mL). The microtubule stability was assessed through microscopic imaging using Olympus microscope equipped with Andor iXON3 897 EMCCD.

4.14. F-Actin Staining of PC12 Derived Neurons Cultured on CFGO Hydrogel. For visualization of F-actin filaments, PC12 cells were first cultured on CFGO-coated surfaces and then differentiated into neurons using NGF for 7 d. Thereafter the cells were fixed with 4% formaldehyde and were stained with 165 nM Alexa Fluor 488 Phalloidin for 20 min at room temperature. Then it was washed twice with PBS; the nucleus was stained with Hoechst dye H33258 (0.05 mg/mL) and observed under Olympus microscope equipped with Andor iXON3 897 EMCCD camera.

4.15. Primary Culture of Rat Cortical Neuron. The culture of primary cortical neurons in this work was performed following a previously described method.[38,39] Briefly, timed-pregnant Sprague−Dawley rats were taken, and brains were isolated from E18 embryos. Then the brain cortices were microdissected, processed, and filtered. Next, to assess the growth response of the cortical neurons on CFGO hydrogel surface, cortical neurons with an initial cell density of 1×10^5 cells/mL were cultured on CFGO-coated surfaces in Neurobasal media supplemented with B27, Pen/Strep, and GlutaMAX for the next 14 d. Each experiment was performed in triplicate, and control experiments were performed simultaneously.

4.16. Immunochemistry Staining of the Cortical Neurons. The neurons cultured on the CFGO hydrogels were identified by staining them with MAP2, a neuronal marker. In brief, the cultured neurons were fixed with 4% formaldehyde, permeabilized with 0.2% Triton X-100, and thereafter incubated with mouse anti-MAP2 overnight at 4 °C. After they were washed with PBS, the neurons were further incubated with fluorescence-labeled secondary goat antimouse for 1 h at 37 °C, and nuclear staining was performed using Hoechst dye H33258 (0.05 mg/mL).

4.17. Live/Dead Cell Assay. For this experiment, freshly prepared CFGO hydrogel was coated on a cover glass slide using spin coater. Then, the primary cortical neurons were plated on the CFGO hydrogel-coated glass surfaces. The neurons were cultured for 14 d. After 14 d of culture, the neurons were treated with a solution

DOI: 10.1021/acschemneuro.8b00514
ACS Chem. Neurosci. XXXX, XXX, XXX−XXX

containing both 2 μM calcein AM and 4 μM PI in the dark. After 30 min, neurons were washed with PBS buffer to remove the excess dye. Finally, live/dead cell status of the cell was revealed through microscopy of the stained cells using Olympus microscope equipped with Andor iXON3 897EMCCD camera.

4.18. Western Blot Analysis. Whole cell extracts were isolated from PC12 cells and rat primary cortical neurons were cultured on CFGO hydrogel were fractionated by SDS poly(acrylamide) gel electrophoresis (PAGE) and transferred to a 0.45 μm PVDF membrane using a transfer apparatus following the manufacturer's protocol (Biorad). After that the membranes were blocked using 5% nonfat milk in a mixture of tris-buffered saline and Tween 20 (TBST) for 1 h and sequentially probed with primary antibodies against GAP 43, Tuj 1, and MAP2. Membranes were washed thrice for 10 min with TBST and incubated with horseradish peroxidase-conjugated antimouse or antirabbit secondary antibodies for 2 h. Blots were again washed thrice with TBST and developed with the ECL system using Luminata Forte Western HRP Substrate. α-Tubulin was used as a protein loading control. All quantitative densitometry analyses of the blots obtained were performed using ImageJ software, and relative expressions represented were normalized to the α-tubulin.

4.19. Animal Models. In our laboratory, we used male pathogen-free C57BL/6 mice (8−11 weeks) for the development of cryogenic injury model. All animal experiments were conducted following the laws and regulations of the regulatory authorities of our Institutional Animal Ethics Committee.

4.20. Cryogenic Injury Model (CIM) and Histological Studies. The cryogenic injury model has been developed following previously described method.[40] Briefly, the mice were divided into three groups (five mice in each group; n = 5). The animals were anaesthetized using 2.5% Avertin injected intraperitoneally at a dosage of 10 mg/mL body weight of the mice and were placed on an elevated platform for the surgery. The hair was shaved and rubbed with ethanol from the head region to disinfect the area. A midline sagittal incision was made to expose the skull of the mice. The bregma and lambda were used as a landmark to mark the left parietal area of the brain for the injury. A cylindrical copper rod of diameter 3.4 mm was dipped in liquid nitrogen prior to the surgery, and the rod was placed on the exposed left parietal skull for ∼60 s to make an injury. Wound was closed using suture needle after the injury. The experimental mice were applied with the gel over the injury prior the wound closure, whereas the sham operated mice were left untreated. All the operated mice were kept for recovery and were sacrificed by transcardial perfusion using 4% formaldehyde at two different time points post injury (5 and 7 d). The brains from traumatized mice were isolated and kept overnight in formaldehyde for postfixation, and then they were processed for histological sections. Coronal brain sections of 5 μm thickness were obtained and stained with Cresyl Violet and GFAP antibody for histological and immunohistological studies, respectively. The reactive astrocytes of the hilus region of DG were counted using ImageJ software program (National Institutes of Health (NIH)). Data are represented as mean ± SD.

4.21. Data Analysis. To analyze various microscopic images, image J software was used. Origin 8.5 pro was used to calculate various spectroscopic data and bar diagram. For statistical analysis, tow tailed Student's t test and one-way ANOVA were performed. In various experiments, statistical values were for $^{*}P \leq 0.03$ and $^{**}P \leq 0.05$.

■ ASSOCIATED CONTENT

Supporting Information

The Supporting Information is available free of charge on the ACS Publications website at DOI: 10.1021/acschemneuro.8b00514.

Figures of synthetic scheme for preparation of 2-hydroxy-*N*′,*N*′,*N*′-trimethylethanaminium, mass spectra of 2-hydroxy-*N*′,*N*′,*N*′-trimethylethanaminium, FT-IR spectra of GO and CFGO, UV spectra of GO and CFGO, XPS spectra of CFGO, illustration of the injectable nature of the CFGO-based hydrogel, expression of GAP 43 protein isolated from PC12-derived neurons at different days cultured on the CFGO-based hydrogel, microscopic images displaying F-actin staining, microscopic images of PC12-derived neurons for neurite outgrowth in different channels, microscopic images of primary cortical neurons in different channels (PDF)

■ AUTHOR INFORMATION

Corresponding Author

*Fax: +91-33-2473-5197/0284. Phone: +91-33-2499-5872. E-mail: sghosh@iicb.res.in.

ORCID

Gaurav Das: 0000-0002-8432-5384

Surajit Ghosh: 0000-0002-8203-8613

Author Contributions

[§]These two authors contributed equally. K.P. performed synthesis, purification, and characterization of CFGO hydrogel. K.P. performed various in vitro assays such as FT-IR, UV, and XPS. G.D. performed all the cell-based assays such as biocompatibility, neurite outgrowth, intracellular microtubule imaging, F-actin staining, and Western blot. J.K., G.D., and V.G. executed the rat primary cortical neuron culture experiment and generated the cryo-injury mice model. G.D. and J.K. performed the immunocytochemistry and histological studies. S.B. and A.S.A. supported K.P. and G.D. for performing various experiments and edited the manuscript. S.G. conceived the idea, supervised the project, and wrote the manuscript.

Notes

The authors declare no competing financial interest.

■ ACKNOWLEDGMENTS

K.P., S.B., and A.S.A. thank UGC fellowship. G.D. thanks ICMR fellowship. V.G. and J.K. thank DST fellowship. We thank Dr. S. Bodhak, CGCRI, for performing the XPS experiment. S.G. kindly acknowledges SERB India for providing financial support (EMR/2015/002230) and CSIR-IICB for financial support (HCP-0012), infrastructure, and animal facility.

■ ABBREVIATIONS

GO, Graphene oxide; CFGO, Acetylcholine-functionalized GO

■ REFERENCES

(1) Glebova, N. O., and Ginty, D. D. (2005) Growth and survival signals controlling sympathetic nervous system development. *Annu. Rev. Neurosci. 28*, 191−222.

(2) Nowakowski, R. S. (2006) Stable neuron numbers from cradle to grave. *Proc. Natl. Acad. Sci. U. S. A. 103*, 12219−12220.

(3) Hua, J. Y., and Smith, S. J. (2004) Neural activity and the dynamics of central nervous system development. *Nat. Neurosci. 7* (4), 327−332.

(4) Qin, W., Bauman, W. A., and Cardozo, C. (2010) Bone and muscle loss after spinal cord injury: organ interactions. *Ann. N. Y. Acad. Sci. 1211*, 66−84.

(5) Thompson, L. M. (2008) Neurodegeneration: a question of balance. *Nature 452*, 707−708.

(6) Lindvall, O., and Kokaia, Z. (2006) Stem cells for the treatment of neurological disorders. *Nature 441*, 1094−1096.

DOI: 10.1021/acschemneuro.8b00514
ACS Chem. Neurosci. XXXX, XXX, XXX−XXX

(7) Schmidt, C. E., and Leach, J. B. (2003) Neural Tissue Engineering: Strategies for Repair and Regeneration. *Annu. Rev. Biomed. Eng. 5*, 293−347.
(8) Hong, Le T. A., Kim, Y. M., Park, H. H., Hwang, D. H., Cui, Y., Lee, E. Mi., Yahn, S., Lee, J. K., Song, S. C., and Kim, B. G. (2017) An injectable hydrogel enhances tissue repair after spinal cord injury by promoting extracellular matrix remodeling. *Nat. Commun. 8*, 1−14.
(9) Malarkey, E. B., Fisher, K. A., Bekyarova, E., Liu, W., Haddon, R. C., and Parpura, V. (2009) Conductive single-walled carbon nanotube substrates modulate neuronal growth. *Nano Lett. 9*, 264−268.
(10) Eigler, S., and Hirsch, A. (2014) Chemistry with graphene and graphene oxide-challenges for synthetic chemists. *Angew. Chem., Int. Ed. 53* (30), 7720−7738.
(11) Kurapati, R., Mukherjee, S. P., Martín, C., Bepete, G., Vázquez, E., Pénicaud, A., Fadeel, B., and Bianco, A. (2018) Degradation of Single-Layer and Few-Layer Graphene by Neutrophil Myeloperoxidase. *Angew. Chem., Int. Ed. 57*, 11722−11727.
(12) Savchenko, A., Cherkas, V., Liu, C., Braun, G. B., Kleschevnikov, A., Miller, Y. I., and Molokanova, E. (2018) Graphene biointerfaces for optical stimulation of cells. *Sci. Adv. 4*, 1−10.
(13) Sun, X., Liu, Z., Welsher, K., Robinson, J. T., Goodwin, A., Zaric, S., and Dai, H. (2008) Nano-Graphene Oxide for Cellular Imaging and Drug Delivery. *Nano Res. 1*, 203−212.
(14) Zhang, Y., Ali, S. F., Dervishi, E., Xu, Y., Li, Z., Casciano, D., and Biris, A. S. (2010) Cytotoxicity effects of graphene and single-wall carbon nanotubes in neural phaeochromocytoma-derived PC12 cells. *ACS Nano 4*, 3181−3186.
(15) Yang, X., Qiu, L., Cheng, C., Wu, Y., Ma, Z. F., and Li, D. (2011) Ordered gelation of chemically converted graphene for next-generation electroconductive hydrogel films. *Angew. Chem., Int. Ed. 50* (32), 7325−7328.
(16) Navarro, X., Krueger, T. B., Lago, N., Micera, S., Stieglitz, T., and Dario, P. J. (2005) A critical review of interfaces with the peripheral nervous system for the control of neuroprostheses and hybrid bionic systems. *J. Peripher. Nerv. Syst. 10*, 229−258.
(17) Buzsaki, G., Bickford, R. G., Ponomareff, G., Thal, L. J., Mandel, R., and Gage, F. H. (1988) Nucleus basalis and thalamic control of neocortical activity in the freely moving rat. *J. Neurosci. 8*, 4007−4026.
(18) Crochet, S., Fuentealba, P., Cissé, Y., Timofeev, I., and Steriade, M. (2006) Synaptic plasticity in local cortical network in vivo and its modulation by the level of neuronal activity. *Cereb Cortex. 16* (5), 618−631.
(19) Hashimoto, M., Kazui, H., Matsumoto, K., Nakano, Y., Yasuda, M., and Mori, E. (2005) Does donepezil treatment slow the progression of hippocampal atrophy in patients with Alzheimer's disease. *Am. J. Psychiatry 162*, 676−682.
(20) O'Neill, M. J., Murray, T. K., Lakics, V., Visanji, N. P., and Duty, S. (2002) The role of neuronal nicotinic acetylcholine receptors in acute and chronic neurodegeneration. *Curr. Drug Targets: CNS Neurol. Disord. 1*, 399−411.
(21) Cooper-Kuhn, C. M., Winkler, J., and Kuhn, H. G. (2004) Decreased neurogenesis after cholinergic forebrain lesion in the adult rat. *J. Neurosci. Res. 77*, 155−165.
(22) Berger-Sweeney, J. (2003) The cholinergic basal forebrain system during development and its influence on cognitive processes: important questions and potential answers. *Neurosci. Biobehav. Rev. 27*, 401−411.
(23) Höhmann, C. F., Brooks, A. R., and Coyle, J. T. (1988) Neonatal lesions of the basal forebrain cholinergic neurons result in abnormal cortical development. *Dev. Brain Res. 42*, 253−264.
(24) Das, S., Moon, H. C., Singer, R. H., and Park, H. Y. (2018) A transgenic mouse for imaging activity-dependent dynamics of endogenous Arc mRNA in live neurons. *Sci. Adv. 4*, 1−14.
(25) Warburton, E. C., Koder, T., Cho, K., et al. (2003) Cholinergic neurotransmission is essential for perirhinal cortical plasticity and recognition memory. *Neuron 38*, 987−996.
(26) Kilgard, M. P., and Merzenich, M. M. (1998) Cortical map reorganization enabled by nucleus basalis activity. *Science 279*, 1714−1718.
(27) Conner, J. M., Chiba, A. A., and Tuszynski, M. H. (2005) The basal forebrain cholinergic system is essential for cortical plasticity and functional recovery following brain injury. *Neuron 46*, 173−179.
(28) Reis, C., Gospodarev, V., Reis, H., Wilkinson, M., Gaio, J., Araujo, C., Chen, S., and Zhang, J. H. (2017) Traumatic Brain Injury and Stem Cell: Pathophysiology and Update on Recent Treatment Modalities. *Stem Cells Int. 2017*, 1−13.
(29) Tu, Q., Pang, L., Wang, L., Zhang, Y., Zhang, R., et al. (2013) Biomimetic choline-like graphene oxide composites for neurite sprouting and outgrowth. *ACS Appl. Mater. Interfaces 5* (24), 13188−13197.
(30) Giano, M. C., Ibrahim, Z., Medina, S. H., Sarhane, K. A., Christensen, J. M., Yamada, Y., Brandacher, G., and Schneider, J. P. (2014) Injectable bioadhesive hydrogels with innate antibacterial properties. *Nat. Commun. 5*, 1−9.
(31) Das, S., Kumar, R., Jha, N. N., and Maji, S. K. (2017) Controlled Exposure of Bioactive Growth Factor in 3D Amyloid Hydrogel for Stem Cells Differentiation. *Adv. Healthcare Mater. 6*, 1−14.
(32) Jana, B., Mondal, G., Biswas, A., Chakraborty, I., Saha, A., Kurkute, P., and Ghosh, S. (2013) Dual functionalized graphene oxide serves as a carrier for delivering oligohistidine- and biotin-tagged biomolecules into cells. *Macromol. Biosci. 13* (11), 1478−1484.
(33) Dent, E. W., and Baas, P. W. (2014) Microtubules in neurons as information carriers. *J. Neurochem. 129* (2), 235−239.
(34) Margulies, S., and Hicks, R. (2009) Combination therapies for traumatic brain injury: prospective considerations. *J. Neurotrauma. 26* (6), 925−939.
(35) Margulies, S., Anderson, G., Atif, F., Badaut, J., Clark, R., Empey, P., Guseva, M., Hoane, M., Huh, J., Pauly, J., Raghupathi, R., Scheff, S., Stein, D., Tang, H., and Hicks, M. (2016) Combination Therapies for Traumatic Brain Injury: Retrospective Considerations. *J. Neurotrauma. 33*, 101−112.
(36) Hummers, W. S., and Offeman, R. E. (1958) Preparation of Graphitic Oxide. *J. Am. Chem. Soc. 80*, 1339−1339.
(37) Adak, A., Das, G., Barman, S., Mohapatra, S., Bhunia, D., Jana, B., and Ghosh, S. (2017) Biodegradable Neuro-Compatible Peptide Hydrogel Promotes Neurite Outgrowth, Shows Significant Neuroprotection, and Delivers Anti-Alzheimer Drug. *ACS Appl. Mater. Interfaces 9*, 5067−5076.
(38) Xu, S. Y., Wu, Y. M., Ji, Z., Gao, X. Y., and Pan, S. Y. A. (2012) Modified Technique for Culturing Primary Fetal Rat Cortical Neurons. *J. Biomed. Biotechnol. 2012*, 1−7.
(39) Beaudoin, G. M. J., Lee, S. H., Singh, D., Yuan, Y., Ng, Y. G., Reichardt, L. F., and Arikkath, J. (2012) Culturing pyramidal neurons from the early postnatal mouse hippocampus and cortex. *Nat. Protoc. 7*, 1741−54.
(40) Raslan, F., Albert-Weißenberger, C., Ernestus, R. I., Kleinschnitz, C., and Sirén, A. L. (2012) Focal brain trauma in the cryogenic lesion model in mice. *Exp Transl Stroke Med. 4*, 1−5.

DOI: 10.1021/acschemneuro.8b00514
ACS Chem. Neurosci. XXXX, XXX, XXX−XXX